









Half-Annular Leaky-Wave Antenna With Suppressed Open Stopband: Design and Experimental Testing

Maksim Kuznetsov , *Student Member, IEEE*, Davide Comite , *Senior Member, IEEE*,
 Symon K. Podilchak , *Member, IEEE*, Paolo Burghignoli , *Senior Member, IEEE*,
 Alessandro Galli , *Member, IEEE*, Al P. Freundorfer , *Senior Member, IEEE*,
 Yahia M. M. Antar , *Life Fellow, IEEE*, and Paolo Baccarelli , *Member, IEEE*

Abstract—A new half-annular bull-eye leaky-wave antenna (LWA) design with suppressed open stopband (OSB) and integrated feeding is presented. The 2-D aperture offers a pencil beam with scanning through broadside and with stable gain values as a function of frequency. To achieve directional radiation, a TM_0 surface wave supported by a grounded dielectric slab is properly perturbed by means of a suitable planar-periodic double-strip aperture. In addition, the proposed structure offers improved performance and reduced design complexity with respect to previous LWAs having a nonsuppressed OSB. Dispersion analyses based on a well-established method-of-moments approach are also performed to characterize the fast spatial harmonic supported by the structure and to determine the size, position, and periodicity of the strips needed for optimal OSB suppression. Simulations and experiments have been carried out to validate the antenna performance against the optimized unit cell. The fabricated planar-periodic LWA also provides continuous beam scanning from -35° to 40° , with a peak realized gain of 21 dBi.

Index Terms—Leaky-wave antenna (LWA), open stopband (OSB), scanning.

I. INTRODUCTION

PLANAR leaky-wave antennas (LWAs) are a class of radiating structure that has received significant interest in the last few decades (see, e.g., [1], [2]). They provide high efficiency, wide-band features, and, depending on the type of design, directive beams with scanning capability, or fixed beams at broadside. Their frequency scanning features are also of interest for tracking, radars, and other sensing applications.

LWAs generally consist of uniform (e.g., slotted waveguide) and quasi-uniform structures, or periodic and controlled surface

wave (SW) perturbations, which are supported by a waveguide (e.g., a grounded dielectric slab). Both 1-D and 2-D designs are possible, whose choice essentially determines beam shape and maximum gain (see, e.g., [3], [4], [5]). Several kinds of unit-cell elements for a periodic LWA are possible. They include printed strips [5], metasurfaces [6], and holes [7]. An overview can be found in [2]. Even if high-gain beams scanning through broadside are possible, when the radiation is supported by the excitation of a fast backward-forward spatial harmonic, LWA performance can be diminished by the presence of an open stopband (OSB). The OSB occurs when the propagation constant of the leaky mode approaches zero (see, e.g., [1], [8]) and determines a drop of the attenuation constant around the frequency corresponding to broadside, resulting in reduced antenna efficiency, deterioration of the Bloch impedance, and reduction of the realized gain [8], [9].

A number of effective solutions have been proposed to reduce [9], [10] and suppress [8], [11], [12] the OSB. Among others, metamaterial-type unit cells have been properly engineered to control the attenuation constant and to eliminate gain reductions [13]. Different loading mechanisms of the unit cells [8] as well as asymmetric construction can also be considered [11], [14], [15]. In this framework, a very simple approach to suppress the OSB can leverage the use of asymmetric unit cells, as theoretically outlined in [12], whose apertures can be constituted by nonidentical elements.

Those preliminary findings [12] are particularly well suited for outlining the 1-D unit cell for 2-D full-annular or half-annular metal strip grating LWAs with suppressed OSB. In this letter, we present the design and the experimental validation of a new half-annular LWA with suppressed OSB, offering minimal gain reduction when scanning across broadside. The geometry is reported in Fig. 1. The antenna is planar and excited by means of a fully integrated feeder; i.e., a surface-wave launcher (SWL) printed within the ground plane [16].

II. THEORETICAL CONSIDERATIONS AND DISCUSSIONS

Radially periodic LWAs can be classified as 2-D LWAs, even if the periodicity develops along one dimension (i.e., the radial one). They are typically excited in the center with azimuth-symmetric or nonsymmetric sources, whose design impacts the beam shape [5], [16]. Off-centered feeding is also possible to achieve unconventional steering [17], [18]. When the source is placed in the center of the structure, a radially propagating wave is excited, which can give rise to conical radiation at a certain angle, or to a broadside pencil beam [5], [19], [20]; both

Manuscript received 21 December 2022; accepted 10 January 2023. Date of publication 12 January 2023; date of current version 5 May 2023. (*Corresponding author: Symon K. Podilchak.*)

Maksim Kuznetsov and Symon K. Podilchak are with the Institute of Digital Communications, University of Edinburgh, Edinburgh EH9 3JW, U.K. (e-mail: mk11@hw.ac.uk; s.podilchak@ed.ac.uk).

Davide Comite, Paolo Burghignoli, and Alessandro Galli are with the Department of Information Engineering, Electronics and Telecommunications, "Sapienza" University of Rome, 00184 Rome, Italy (e-mail: davide.comite@uniroma1.it; paolo.burghignoli@uniroma1.it; alessandro.galli@uniroma1.it).

Al P. Freundorfer and Yahia M. M. Antar are with the Royal Military College of Canada, Kingston, ON K7K 7B4, Canada, and also with the Queen's University, Kingston, ON K7K 7B4, Canada (e-mail: freund@queensu.ca; antar-y@rmc.ca).

Paolo Baccarelli is with the Department of Industrial, Electronic, and Mechanical Engineering, Roma Tre University, 00146 Rome, Italy (e-mail: paolo.baccarelli@uniroma3.it).

Digital Object Identifier 10.1109/LAWP.2023.3236614

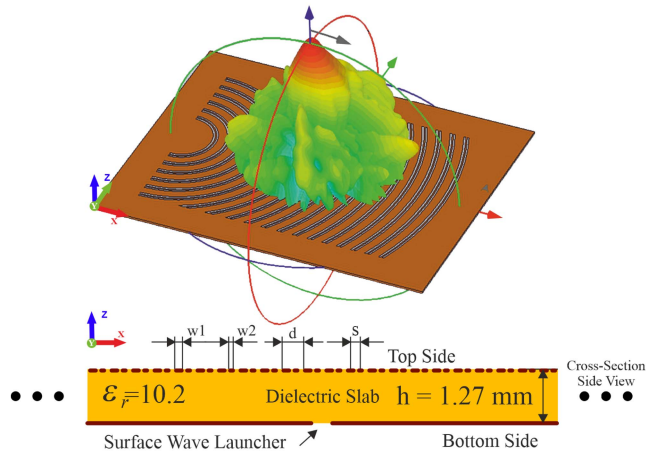


Fig. 1. Perspective and side views of the proposed planar LWA on a single-layer GDS. Nineteen double strip lines constitute the top aperture, whereas the bottom ground plane has an integrated feeder; i.e., a surface wave launcher (SWL) with a 50Ω input feeding line, defined by a coplanar waveguide.

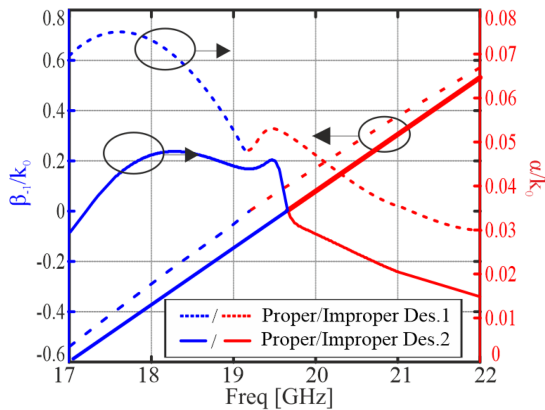


Fig. 2. Normalized phase (β_{-1}/k_0) and attenuation (α/k_0) constant for designs 1 and 2 (see dimensions in Table I).

cases are supported by the excitation of a fast backward spatial harmonic. Thanks to the azimuthal symmetry of the annular rings (or similarly half-annular structure), the dispersion features of the leaky mode can be analyzed by studying the unit cell of the corresponding and linearized 1-D version (e.g., by assuming $k_\rho = k_x$). The same approach was exploited and experimentally validated in [9], [16], and [21].

Half-annular or one-sided 2-D bull-eye LWAs, in conjunction with directional feed systems, are able to produce a one-sided pencil-beam with continuous-frequency scanning through broadside. They typically suffer, however, from the presence of an OSB that can strongly reduce the radiative performance around broadside. Here, in this letter, a double-strip configuration, which well matches the geometry constraint of the annular antenna and SWL feeder, is used to completely suppress the OSB. The dispersion analysis is achieved by means of an in-house approach [22], particularly suited to optimize a nonsymmetric unit cell constituted by two strips.

Previous designs [9] (see Fig. 5) and [10] (see Fig. 2), showed that the OSB effects can be mitigated, but not suppressed if using a multilayered structure. The very simple approach proposed herein differs from [9], [10]: it exploits a single-layer grounded

TABLE I
PROPOSED ANTENNA DIMENSIONS FOR OSB SUPPRESSION [MM]

Design Type	Strip 1 w_1	Strip 2 w_2	Periodicity d	Distance s
Design 1	1.2	0.96	8	1.9
Design 2	1	0.8	8	1.9

dielectric slab (which is desirable to reduce dielectric losses, design complexity, and manufacturing costs) to fully suppress the OSB. In particular, a simple introduction of an additional strip within the unit cell is employed to achieve the desired asymmetry as follows [12]. By properly sizing the two strips (whose number can be generally increased to add degrees of freedom, to a certain extent), it is also possible to control the attenuation constant (i.e., to tune gain/efficiency). Two different unit-cell designs are proposed here; i.e., designs 1 and 2, and the corresponding dimensions can be found in Table I.

The optimized dispersion characteristics for both designs, performed using an in-house method-of-moments (MoM) approach [22], to extract the TM leaky mode for a fast $n = -1$ spatial harmonic, are reported in Fig. 2. The frequencies at which broadside radiation occurs (i.e., where the phase constant is equal to zero and the leaky mode changes from the backward to the forward propagation regime) for design 1 is around 19.1 GHz while for design 2 is 19.4 GHz. A very minor variation for α can be observed, as can occur in similar optimized structures [8]. However, values for α in Fig. 2 are well above zero around broadside, thus definitively showing the desired OSB suppression. This is in contrast to previous single-strip and dual-layer LWAs where $\alpha = 0$ when $\beta \approx 0$ for broadside radiating frequencies (see, e.g., [10] and [16]).

In the following, we select design 1 (see Table I) for further study and experimental testing, mainly, due to the higher values for the leakage constant. This important feature can provide good values for the leaky radiation efficiency while also keeping the antenna more compact [1], [2]. As well known, the solution to the modal problem is related to an infinite structure, which can have an undetermined number of unit cells. The leaky-mode wavenumber supported by the bidirectional structure is described by exactly the same phase and attenuation constant if the propagation is either along the positive direction of the x -axis in Fig. 1 or along the negative one, even in the presence of asymmetric perturbations [23]. This is not the case with the Bloch impedance: due to the asymmetry of the adopted unit cell, two different impedances Z_B^\pm are reported in Fig. 3. These results have been achieved by means of a full-wave solution for a truncated structured, as outlined in [10] and references therein, for the Bloch waves traveling in both the positive and negative x -directions.

As concerns the Bloch impedance behavior around the broadside radiating frequencies [8], we observe in Fig. 3 that Z_B^+ presents the desired smooth trend and, therefore, is more amenable to antenna source impedance matching for both the real and imaginary parts. This behavior is made possible thanks to the suppression of the OSB [8], clearly indicating that the desired Bloch mode should propagate along the positive x -direction. This suggests to design an LWA whose aperture presents first the wide and then the narrow strip moving along increasing x values. This is visible in Fig. 4, and within the relevant inset, which shows a cross-section view of the

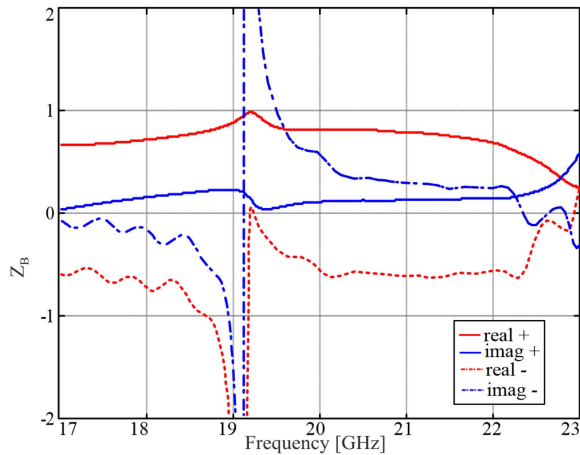


Fig. 3. Bloch impedance for the unit cell considering design 1. The plus and negative superscripts indicate the two possible feeding approaches (w_1 or w_2 first) for the incident traveling-wave with respect to the x -axis in Fig. 1.

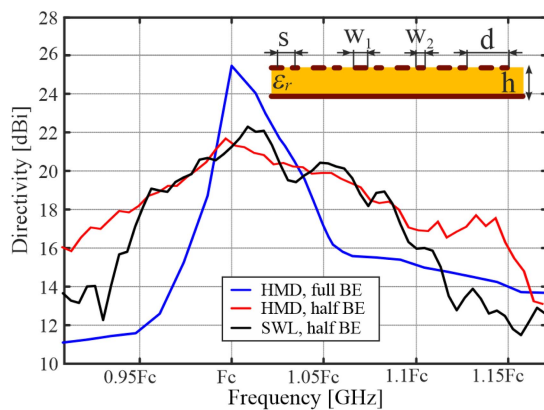


Fig. 4. Simulated directivity of a double-strip antenna considering a full-annular design (i.e., a full BE) and a half-annular design (i.e., half BE) with two different feeders as specified within the legend.

double-strip aperture. Z_B^- , instead, shows rapid and strong variations with a null of the real part exactly at the broadside radiating frequency. Such strong variations are similar to those expected for a symmetric unit cell, like a single strip, as in the inset of Fig. 5 (all results not reported due to space limitations).

III. SIMULATIONS AND DISCUSSIONS

To analyze and discuss the functioning principle of the half-annular antenna with respect to the annular bull-eye, full-wave simulations using state-of-the-art commercial software were performed, considering both the double- and single-strip unit-cell arrangement. Two different feeding mechanisms are also compared: an ideal horizontal magnetic dipole, implemented by etching a subwavelength slot in the ground plane, and an SWL, i.e., a directive coplanar Yagi-Uda configuration (with planar reflectors to direct the power) [24], designed *ex-novo* here to optimize the matching (see Figs. 4–6). The SWL produces a TM_0 SW mode, which will be perturbed by the asymmetric strips without introducing the OSB. The supporting grounded dielectric slab is constituted by a commercial laminate (i.e., Rogers 6010) with rated permittivity $\epsilon_r = 10.2$ and a thickness

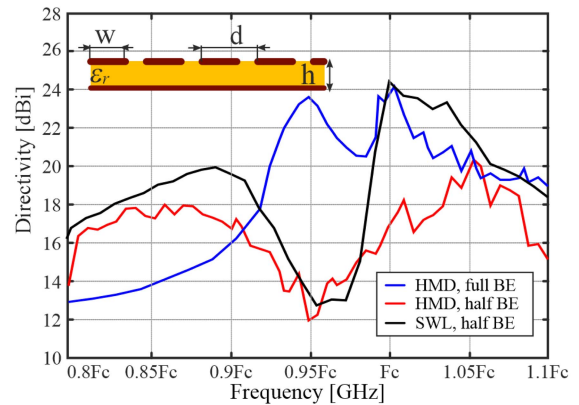


Fig. 5. As in Fig. 4 but with a single-strip unit cell ($w = 1$ mm, $d = 8$ mm).

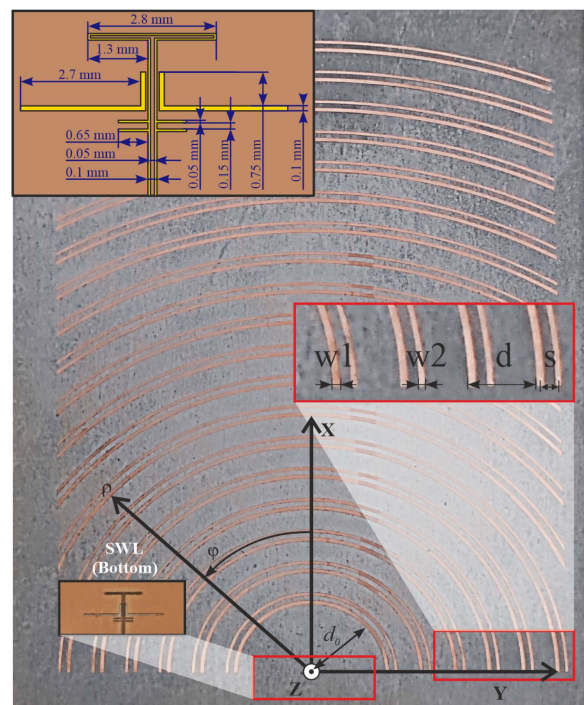


Fig. 6. Manufactured LWA defined by 19 unit cell double strips (top) and the SWL feeder printed on the bottom side, shown in the picture inset.

of 1.27 mm. The choice of a relatively high ϵ_r was made to ensure efficient SW excitation by means of the fully integrated and planar SWL antenna source [24].

The maximum value of the simulated directivity versus the normalized broadside frequency F_c , considering the double-strip configuration, is reported in Fig. 4. The annular antenna (i.e., the full BE) reports some variation of the gain far from the backward/forward transition region, as expected the beam being conical (but nonomnidirectional). It coalesces, instead, in a pencil beam when $|\beta| \leq \alpha$. The simulated broadside radiation occurred around 18.6 GHz. The half-annular design (i.e., half-BE), shows a more stable gain versus frequency, as expected it is pencil-like (similar to Fig. 1); i.e. it scans from approximately backward endfire to forward endfire. The single-strip designs in Fig. 5, instead, shows a strong gain drop close to the normalized broadside frequency, for all cases and especially the

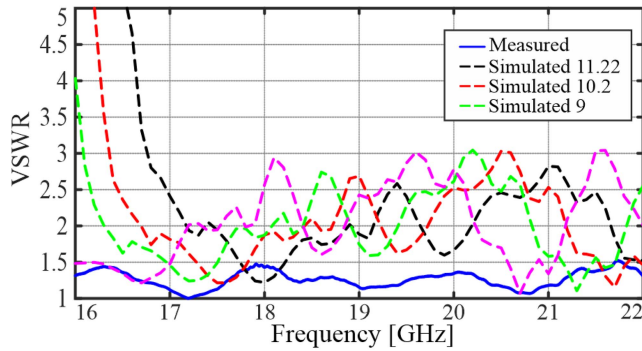


Fig. 7. Measured and simulated 50 Ω matching for the proposed LWA.

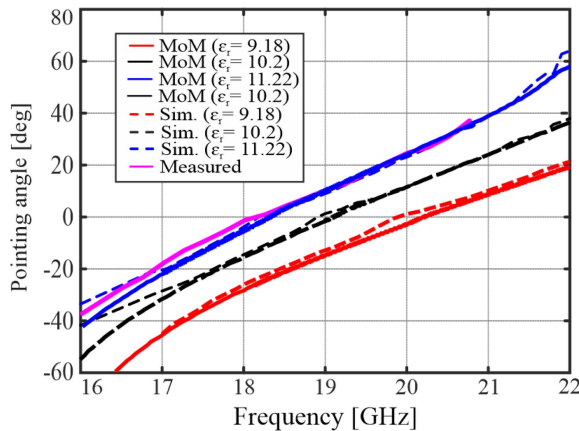


Fig. 8. Comparison of measured, simulated, and theoretical MoM pointing angles, given by $\theta_p = \sin^{-1}(\beta_{-1}/k_0)$, for different substrate permittivities.

half-annular LWA, due to the presence of the OSB, which is instead suppressed in Fig. 4.

IV. MEASUREMENTS AND DISCUSSIONS

The manufactured antenna consists of 19 unit cells and with the feeder etched within the ground plane (see Fig. 6 and the relevant inset). The position of the SWL was optimized to improve the matching while also adjusting its position to the most internal ring [24] (distance $d_0 = 17.4$ mm in Fig. 6).

A 50 Ω picoprobe [25] was calibrated and then connected to the CPW line, for impedance matching measurements. A comparison of the simulated and measured voltage standing wave ratio is reported in Fig. 7, and values are well below 1.5 from 16 to 22 GHz implying minimal reflections.

The simulated beam angle θ_p , the measured, and the theoretical values are reported in Fig. 8. Also, as shown in Figs. 7 and 8, simulations are given for different values of the substrate relative permittivity to consider possible manufacturing tolerances [26]. This is because Rogers 6010, as reported in [26] and [27], can have a practical shift in the dielectric constant. Thus, additional simulations and theoretical studies were completed to anticipate such a shift. Basically, a minor shift in the main beam angle with respect to frequency can be observed, and this is most likely related to the noted relative dielectric tolerances for the PCB material. For instance, the unit cell and LWA structure were designed with a substrate considering $\epsilon_r = 10.2$, but it is most likely closer to 11.2. A comparison between simulated

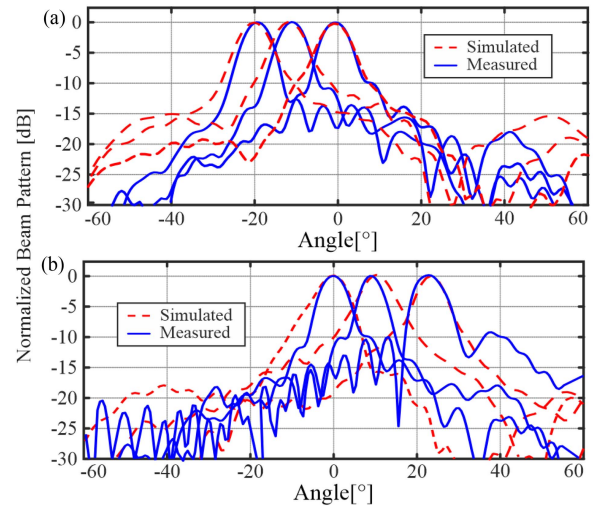


Fig. 9. Patterns (xz -cut): (a) At 17, 17.5, and 18 GHz; (b) 18.1 (broadside), 19, and 20 GHz. A 3-D simulated broadside beam is also shown in Fig. 1.

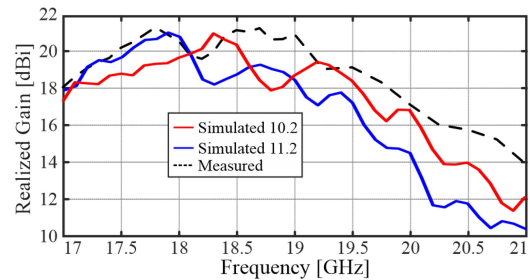


Fig. 10. Simulated and measured maximum realized gain versus frequency.

($\epsilon_r = 11.2$) and measured patterns, in the xz -plane (see Fig. 1), are also in Fig. 9.

Realized gain maxima versus frequency are in Fig. 10. The slight gain drop of about 2 dB, visible from about 18 to 18.5 GHz, is related to some minor loss in the desired TM SW power. Similar findings were shown in Fig. 4 for the directivity with the SWL. This response is due to the generation of unwanted TE SW power or azimuthal ring currents on the printed metallic rings (similarly as observed in [9] and [24]). Cross-polarization levels (not reported for space limitations) are -10 dB (or below) and the simulated total antenna efficiency reaches 90%.

V. CONCLUSION

A double-strip half-annular, radially periodic, compact LWA with suppressed OSB, improved performance, and significantly lower complexity (with respect to the design in [10]), is presented. In particular, a simple and asymmetric unit cell based on a single-layer dielectric slab, suitable for designing a planar bull-eye LWA, has been considered. A pencil beam offering stable realized gain when scanning across broadside has been achieved and experimentally tested, outperforming previous LWAs with nonsuppressed OSBs. The antenna feeder is fully integrated within the ground plane, offering broadband 50 Ω impedance matching. Also, the proposed LWA can represent an attractive, simple, and compact solution for remote sensing, tracking, and wireless power transfer applications, where stable scanning beams are desired.

REFERENCES

- [1] D. R. Jackson, C. Caloz, and T. Itoh, "Leaky-wave antennas," *Proc. IEEE*, vol. 100, no. 7, pp. 2194–2206, Jul. 2012.
- [2] D. R. Jackson and A. A. Oliner, *Leaky-Wave Antennas*. Hoboken, NJ, USA: Wiley, 2008, ch. 7, pp. 325–367. [Online]. Available: <https://onlinelibrary.wiley.com/doi/abs/10.1002/9780470294154.ch7>
- [3] G. Mishra and S. K. Sharma, "A multifunctional full-polarization reconfigurable 28 GHz staggered butterfly 1-D-beam steering antenna," *IEEE Trans. Antennas Propag.*, vol. 69, no. 10, pp. 6468–6479, Oct. 2021.
- [4] D. K. Karmokar, S.-L. Chen, D. Thalakituna, P.-Y. Qin, T. S. Bird, and Y. J. Guo, "Continuous backward-to-forward scanning 1-D slot-array leaky-wave antenna with improved gain," *IEEE Antennas Wireless Propag. Lett.*, vol. 19, no. 1, pp. 89–93, Jan. 2020.
- [5] D. Comite et al., "Planar antenna design for omnidirectional conical radiation through cylindrical leaky waves," *IEEE Antennas Wireless Propag. Lett.*, vol. 17, no. 10, pp. 1837–1841, Oct. 2018.
- [6] W. E. I. Liu, Z. N. Chen, and X. Qing, "Broadband low-profile l-probe fed metasurface antenna with TM leaky wave and TE surface wave resonances," *IEEE Trans. Antennas Propag.*, vol. 68, no. 3, pp. 1348–1355, Mar. 2020.
- [7] D. Nagaraju and Y. K. Verma, "A compact conformal stub-loaded long slot leaky-wave antenna with wide beamwidth," *IEEE Antennas Wireless Propag. Lett.*, vol. 20, no. 6, pp. 953–957, Jun. 2021.
- [8] S. Paulotto, P. Baccarelli, F. Frezza, and D. R. Jackson, "A novel technique for open-stopband suppression in 1-D periodic printed leaky-wave antennas," *IEEE Trans. Antennas Propag.*, vol. 57, no. 7, pp. 1894–1906, Jul. 2009.
- [9] D. Comite et al., "Analysis and design of a compact leaky-wave antenna for wide-band broadside radiation," *Sci. Rep.*, vol. 8, no. 1, pp. 1–14, 2018.
- [10] D. Comite et al., "A dual-layer planar leaky-wave antenna designed for linear scanning through broadside," *IEEE Antennas Wireless Propag. Lett.*, vol. 16, pp. 1106–1110, 2016.
- [11] S. Otto, A. Al-Bassam, A. Rennings, K. Solbach, and C. Caloz, "Transversal asymmetry in periodic leaky-wave antennas for Bloch impedance and radiation efficiency equalization through broadside," *IEEE Trans. Antennas Propag.*, vol. 62, no. 10, pp. 5037–5054, Oct. 2014.
- [12] P. Baccarelli, P. Burghignoli, D. Comite, W. Fuscaldo, and A. Galli, "Open-stopband suppression via double asymmetric discontinuities in 1-D periodic 2-D leaky-wave structures," *IEEE Antennas Wireless Propag. Lett.*, vol. 18, no. 10, pp. 2066–2070, Oct. 2019.
- [13] W. Cao, Z. N. Chen, W. Hong, B. Zhang, and A. Liu, "A beam scanning leaky-wave slot antenna with enhanced scanning angle range and flat gain characteristic using composite phase-shifting transmission line," *IEEE Trans. Antennas Propag.*, vol. 62, no. 11, pp. 5871–5875, Nov. 2014.
- [14] X.-L. Tang et al., "Continuous beam steering through broadside using asymmetrically modulated Goubau line leaky-wave antennas," *Sci. Rep.*, vol. 7, 2017, Art. no. 11685.
- [15] J. Liu, W. Zhou, and Y. Long, "A simple technique for open-stopband suppression in periodic leaky-wave antennas using two nonidentical elements per unit cell," *IEEE Trans. Antennas Propag.*, vol. 66, no. 6, pp. 2741–2751, Jun. 2018.
- [16] S. K. Podilchak, P. Baccarelli, P. Burghignoli, A. P. Freundorfer, and Y. M. M. Antar, "Analysis and design of annular microstrip-based planar periodic leaky-wave antennas," *IEEE Trans. Antennas Propag.*, vol. 62, no. 6, pp. 2978–2991, Jun. 2014.
- [17] U. Beaskoetxea, S. Maci, M. Navarro-Cia, and M. Beruete, "3-D-printed 96 GHz bull's-eye antenna with off-axis beaming," *IEEE Trans. Antennas Propag.*, vol. 65, no. 1, pp. 17–25, Jan. 2017.
- [18] D. Comite et al., "Directive 2-D beam steering by means of a multipoint radially periodic leaky-wave antenna," *IEEE Trans. Antennas Propag.*, vol. 69, no. 5, pp. 2494–2506, May 2020.
- [19] A. Ip and D. R. Jackson, "Radiation from cylindrical leaky waves," *IEEE Trans. Antennas Propag.*, vol. 38, no. 4, pp. 482–488, Apr. 1990.
- [20] D. Zhang et al., "Hybrid TM/TE cylindrical leaky waves: Electromagnetic radiation at broadside from radially periodic structures," *IEEE Trans. Antennas Propag.*, vol. 70, no. 3, pp. 1683–1693, Mar. 2022.
- [21] P. Baccarelli et al., "Modal properties of surface and leaky waves propagating at arbitrary angles along a metal strip grating on a grounded slab," *IEEE Trans. Antennas Propag.*, vol. 53, no. 1, pp. 36–46, Jan. 2005.
- [22] P. Baccarelli, S. Paulotto, and C. Di Nallo, "Full-wave analysis of bound and leaky modes propagating along 2D periodic printed structures with arbitrary metallisation in the unit cell," *Microw. Antennas Propag.*, vol. 1, no. 1, pp. 217–225, 2007.
- [23] D. Pisssoort and F. Olyslager, "Study of eigenmodes in periodic waveguides using the Lorentz reciprocity theorem," *IEEE Trans. Microw. Theory Techn.*, vol. 52, no. 2, pp. 542–553, Feb. 2004.
- [24] S. K. Podilchak, P. Baccarelli, P. Burghignoli, A. P. Freundorfer, and Y. M. M. Antar, "Optimization of a planar 'bull-eye' leaky-wave antenna fed by a printed surface-wave source," *IEEE Antennas Wireless Propag. Lett.*, vol. 12, pp. 665–669, 2013.
- [25] "GGB picoprobe model 40a high performance microwave probes," 2022. [Online]. Available: <https://www.lambdaphoto.co.uk/picoprobe-40a-high-performance-microwave-probes.html>
- [26] Rogers Corporation, "General information of dielectric constant for RT/duroid® 6010.2LM and RO3010™ high frequency circuit materials," 2010. [Online]. Available: <https://rogerscorp.com/-/media/project/rogerscorp/documents/advanced-electronics-solutions/english/electrical-design-data/general-information-of-dielectric-constant-for-rt-duroid-6010.pdf>
- [27] M. V. Kuznetsov, V. Gómez-Guillamón Buendía, Z. Shafiq, L. Matekovits, D. E. Anagnostou, and S. K. Podilchak, "Printed leaky-wave antenna with aperture control using width-modulated microstrip lines and TM surface-wave feeding by SIW technology," *IEEE Antennas Wireless Propag. Lett.*, vol. 18, no. 9, pp. 1809–1813, Sep. 2019.